Water Clustering in Polyvinyl Butyral (PVB): Evidenced by Diffusion and Sorption Experiments

C. Arauz-Moreno, K. Piroird, Elise Lorenceau

Water clustering in Polyvinyl butyral (PVB) evidenced by diffusion and sorption experiments

C. Arauz Moreno,*,†,‡ K. Piroird,‡ and E. Lorenceau†

†*Univ. Grenoble Alpes, CNRS, LIPhy, F-38000 Grenoble, France*

‡*Saint-Gobain Recherche, 39 quai Lucien Lefranc, F-93360,Aubervilliers, France*

E-mail: c.arauz_moreno@icloud.com

Abstract

Polyvinyl butyral (PVB) is a transparent amorphous polymer often used to protect fragile surfaces such as glass or photovoltaic panels. The polymer is then packaged in the form of adhesive sheets and bonded to the surfaces. The transport and retention of water in PVB are crucial properties to understand, as they modulate the polymer's adhesion properties. In this work, we propose a detailed experimental study of water diffusion and sorption in PVB over a wide range of temperatures and humidity levels in the surrounding atmosphere. Using spectroscopic and gravimetric measurements, our study elucidates how the diffusion coefficient varies with temperature or vapour concentration, and provides the activation energy for this process. In addition, Dynamic Vapour Sorption (DVS) experiments reveal i) a strong dependence of sorption on hydroxyl group (-OH) concentration and ii) that the solubility of vapour in PVB decreases with temperature. This enables us to trace the heat of solution of water in PVB. A comparison of the thermodynamic data obtained with those for water in volume and with the ENSIC model (Engaged Species Induced Clustering), supports the microscopic view of water organization in PVB in the form of clusters induced by hydrogen bounding.

Introduction

Polyvinyl butyral (PVB) is an amorphous polymer used in composite muti-layered assemblies. Examples include laminated safety glass or photovoltaic (PV) modules. In both applications, the PVB polymer—in the form of a thin sheet—is used to bond two layers of glass together in a sandwich-like geometry while guaranteeing optical transparency. In safety glass, PVB guarantees that if the sandwich is broken, the glass remains attached therewith. This remarkable property can save lives when used in a car windshield. In PV modules, the PVB layer additionally encapsulates the solar cells to protect them from the outside environment, most notably, against water ingress.

Over time, sandwich assemblies with PVB can develop bubbles or blisters, the likelihood being determined destructively via so-called bake or aging tests at elevated temperatures (see norm EN ISO 12543-4 for glass bake testing and standard IEC61215 for the aging of PV modules). The appearance of bubbles or blisters in such tests may be attributed to the amount of water initially dissolved in the PVB bulk,[1] or that which enters the sandwich via the exposed (lateral) edges.[2] In addition to bubble formation, water affects the level of adhesion between the PVB sheet and the glass layers,[3] lowers the polymer's glass transition temperature,[4] and decreases the polymer's stiffness.[5] Thus, a thorough understanding of water transport in PVB is necessary to guarantee optimal and reliable designs of glass products with PVB.

While there is extensive literature on PVB and water transport,[6–9] a brief survey reveals inconsistent estimates in terms of sorption levels, diffusion coefficients, activation energies, as well as a limited availability of high-temperature data. This situation is further complicated given the wide array of commercially available formulations of PVB.

In this study, we explored PVB's transport properties for water, in particular diffusion and sorption for several temperatures and humidity levels. We focused our efforts on RB41– an industrial blend of PVB produced by Eastman that is a staple of glass applications for buildings. By using gravimetric and spectrometry techniques, we show that water diffusion

in PVB is both concentration and temperature dependent. The activation energy for the diffusion process appears non-constant in the range of 25-140°C, with an apparent inflection at around ∼72-75°C. Given the absence of a phase transition for water in this range, the inflection may reflect a change in the polymer itself, such as the transition from the rubbery to the viscous state. We use characteristic times of the polymer to show that this is indeed the case. Regarding sorption, DVS experiments with powder PVB demonstrate a strong dependence of hydroxyl group (-OH) concentration and water sorption with the isotherms being highly non-linear. Our experiments with the sheet incarnation of the polymers reveals that water vapour solubility decreases when increasing the temperature. Remarkably, the loss in solubility is perfectly matched by the increasing vapour pressure of water, resulting in isotherms that are temperature independent when plotted against water vapor chemical activity regardless of the complex structure of the polymer. When taken together, our diffusion and sorption experiments suggest that water transport in PVB is governed by a clustering mechanism, wherein water molecules interact greatly with one another. We propose a qualitative picture, backed by quantitative experiments, where hydrogen bonding is the driving force.

Materials & Methods

As mentioned in the introduction, the PVB studied here comprised RB41 from Eastman. Presentation wise, the PVB film took the form of a thin sheet having a nominal thickness of 760 μm with a surface roughness of approximately 40 μm. The chemical composition included 1-2%wt of vinyl acetate (VAc) units, 18-20%wt vinyl alcohol (VOH) units, and 80%wt of vinyl butyral (VB) units. The blend further included triethylene glycol di-(2-ethylhexanoate) as a plasticizer molecule in a concentration of about 20%wt.[10] The polydispersity index is 1.4, the molar mass is 200 kg mol^{-1}, and the glass transition temperature is around 25°C.[11]

To better comprehend the link between sorption and polymer chemistry, we further sur-

veyed pure PVB in powder form without the plasticizer molecule. In this case, we procured powder having 8%wt and 18%wt vinyl alcohol from Chang Chun Petrochemicals (CCP). The chemical composition was confirmed by nuclear magnetic resonance following the protocol established in.[12]

Diffusion

Diffusion constants were obtained using two techniques: dynamic vapor sorption (DVS), and near-infrared (NIR) spectroscopy. Below, we describe both techniques in detail.

Dynamic Vapor Sorption

The experiments were carried out in a DVS-intrinsic machine from Surface Measurement Systems (SMS). In here, the PVB sample was placed atop a high precision scale (res. $\pm 0.1\mu$m) inside a sealed nitrogen chamber. The machine automatically regulated the chemical activity of water vapor in the atmosphere by mixing dry nitrogen with water from a built-in reservoir while simultaneously recording the change in PVB mass. From the transient uptake of mass, the diffusion coefficient is directly obtained. The working temperature range of the machine was 20°C to 40°C (res. ± 0.2°C).

For our DVS experiments, we assumed the chemical activity of water vapour, a, complied with an ideal gas behavior wherein

$$a = \frac{p_w}{P_{Sat}(T)} \tag{1}$$

where p_w is the partial pressure of water vapour in the controlled atmosphere, and P_{Sat} is the saturation pressure at a given temperature T.

Figure 1(a) depicts an example of a full DVS run at 25°C. The total experiment time was approximately 10 days. The protocol began with an initial segment at $a = 0$ intended to dry the PVB sample, thus generating a baseline mass. This step lasted 2×10^3 mins ($\sim$33 hrs). The activity was then varied in steps of $\Delta a = 0.10$ up to $a = 0.9$, and then downwards

back to $a = 0$ to test for hysteresis. At each step, the mass reached a steady value. A second run was performed at 40°C using a new sample.

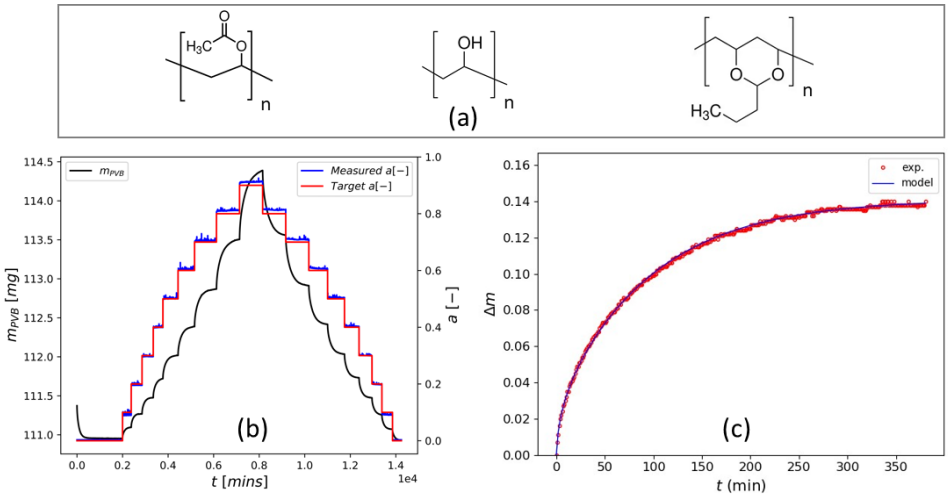

Figure 1: (a) : Chemical structure of the PVB with its different monomer units - left: Vinylacetate - middle : Vinylalcohol -right : Vinylbutyral. (b) : DVS experiment at 25°C showing sorption and desorption kinetics of water vapor in PVB. The blue and red lines correspond respectively to the chemical activity measured and imposed in the chamber, while the black line corresponds to the mass of the PVB sample measured gravimetrically. (c): Sample fit (in blue) of the diffusion equation to the transient PVB mass data (in red) at a=0.10.

To obtain the diffusion coefficient of water in PVB, we fitted the diffusion equation to the transient data, i.e., at each activity level we take $\frac{\partial c}{\partial t} = D\Delta c$, where c is the concentration, D is the diffusion coefficient, and t is the diffusion time. For the fit, the diffusion coefficient was assumed as constant for each sorption step.[13] Figure 1(b) shows a sample computation of the sorption step at $a = 0.10$. For this particular case,we found $D \sim 1.01 \times 10^{-11}$ m^2/s.

Near-infrared (NIR) Spectroscopy

To determine diffusion coefficients at higher temperatures than otherwise allowed by the DVS machine, we were inspired by the FTIR spectroscopy technique developed by Kapur et al.[14] to measure water non-destructively in thin polymeric samples when autoclaved in

between two layers of glass. In this technique, it suffices to measure the ratio r of water-to-polymer absorption peaks and interconverting this metric to the quantitative amount of water dissolved in the polymer by means of a calibration curve. Figure 1 in their paper reveals a reference carbon peak for PVB between 1600 nm and 1720 nm. Meanwhile, the moisture peak was located in between two minima at 1880 nm and 1990 nm.

The experimental protocol developed in this work includes several differences from the technique of Kapur et al. [14] First, we developed an experimental NIR-based set-up for measuring moisture profiles in glass/polymer/glass samples. Second, we streamlined the glass/polymer/glass sample preparation process by suppressing the autoclaving step to limit water loss from samples during this step as demonstrated below. Third, we took additional steps to guarantee an initial homogeneous moisture profile in the samples by routinely verifying the moisture content spatially over a period of several weeks. Finally, we devised a different experimental protocol to induce water diffusion in the PVB layer. All these new implementations are described in detail below.

As illustrated in Figure 2, the set-up included two translation stages. A first motorized stage (x-stage) from Thorlabs (LTS300/M, working range of 300 mm, res. $\pm 5\mu$m), and a second, manual z-stage (25 mm range) having a dedicated holder for a glass sample. With the two translation stages, glass samples with polymers could be scanned in two dimensions with great precision and reproducibility. Meanwhile, the spectrometry readings were obtained by means of a NIRQuest spectrometer (Ocean Optics, 900 nm - 2100 nm, res. 4.8 nm). The readings were taken in reflectance using a tungsten halogen source (360 nm - 2400 nm). The light passed through the sample and was reflected back to the spectrometer using a PTFE white diffuser (reflectivity $\geq$95%) via a bifurcated 400 μm optical fiber probe.

In terms of sample preparation, our raw materials consisted in two layers of float glass (10 cm x 10 cm x 2 mm) covering a single PVB sheet. The glass was washed with a solution of deionized (DI) water and a special glass detergent, namely RBS50 from Sigma-Aldrich. Meanwhile, the PVB was dust-off with a nitrogen gun (5 bar) and conditioned inside a

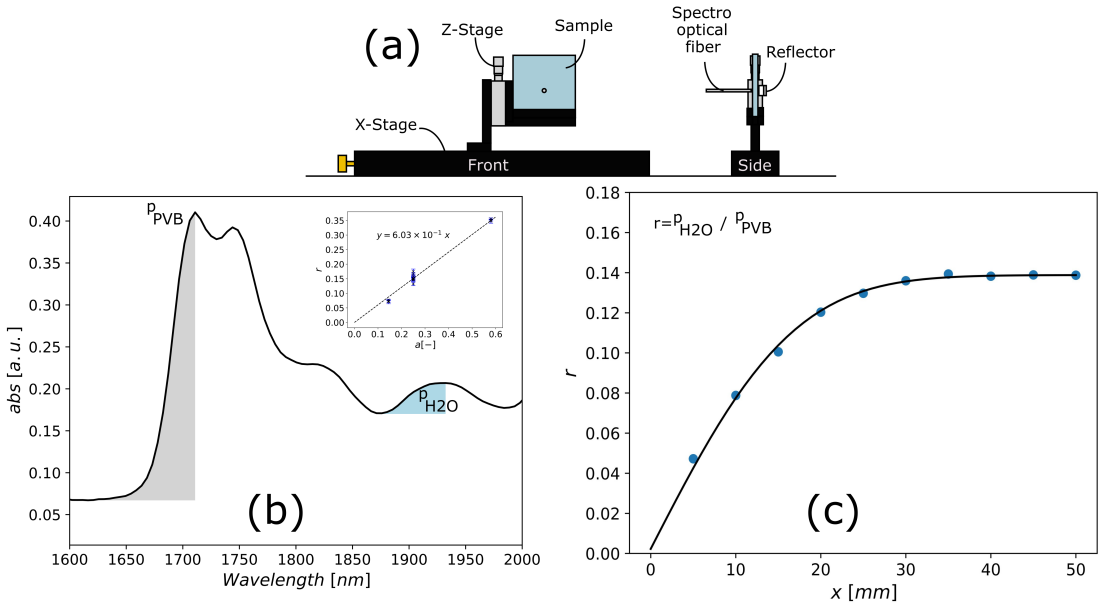

Figure 2: (a) Sketch of the NIR set-up for measuring moisture in glass samples with PVB, (b) Light spectrum defining the absorption peaks (shaded regions) for PVB (grey) and dissolved H_2O (light blue), inset is the Spectro calibration for water absorption in PVB showing r, the ratio of water and PVB absorption peaks versus water vapor activity during conditioning, (c) Sample diffusion profile in a pre-press after heating inside an oven for 16hrs at 140°C, showing r versus PVB absorption peaks as a function of the distance from the surrounding atmosphere. The solid line is the diffusion model given by eq. (2).

climatic cabinet at $a = 0.25$ for at least one week unless noted otherwise. The polymer and glass layers were subsequently bonded together by slight heating in a convection oven (15-30 mins at 90°C) followed by the application of a small pressure load via a nip-roll calender (EMS-650). No autoclaving was employed. The resulting samples, herein referred to as a pre-press (we borrow this term from the industrial nomenclature of safety glass production), were optically hazy due to interfacial air trapped in the polymer roughness.

Figure 2 (b) shows a sample spectrum reading for a pre-press wherein the shaded regions define the absorption peaks for PVB (grey) and water (light blue). As a background reference, we took a single glass lite having a thickness equivalent to that of the pre-press samples (thickness ∼5 mm). The height of the peaks were determined by subtracting the absorption values of the maxima and minima of the shaded regions. For reference, from 40 measurements spread across different locations in four separate samples, we found the PVB peak to be constrained on average between 1609 nm - 1710 nm, while the water peak was around 1873 nm - 1925 nm. The standard deviation of the wavelengths did not exceed 4.5 nm, which is the minimum resolution of the spectrometer. Note that this method is not totally rigorous for water, since the baseline is estimated by taking into account the absorption minimum around 1875 nm and omitting that at 1980 nm. However, we have verified that this approximation results in an error of less than 10%.

Since the pre-press is translucent, the spectra readings were found to be vertically shifted depending on the local haze as depicted in Figure 3(a). This vertical shift, however, bore no impact on the determination of water content as measured by r, the ratio of the water and PVB absorption peaks. In comparison to the pre-press, the spectra readings formed a single curve in a fully transparent (autoclaved) glass sample as demonstrated by Figure 3(b). However, a noticeable drop in the size of the water peak is observed around the samples' edge, thus suggesting that water was lost during high-temperature autoclaving. This observation led us to omit the hight-temperature autoclaving step to ensure that the polymer's water content was maintained during the process.

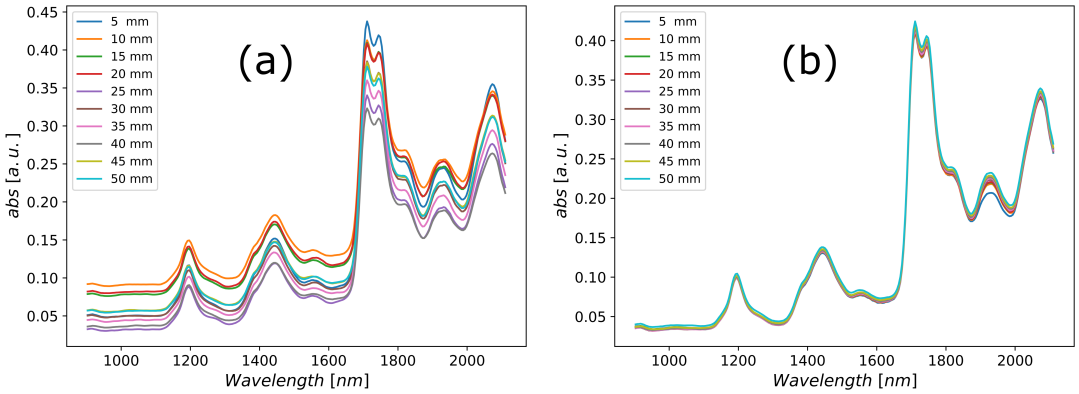

Figure 3: Spectra readings as a function of spatial location in the midsection of a glass sample. The sample's edge is at x=5mm, whereas the center is at x=50mm. (a) Spectra from a pre-press. The inherent haziness variability of the sample shifts the spectral readings vertically. (b) Spectra from an autoclaved sample overlap onto a single curve, except at the edge (x=5mm) around the moisture peak suggesting that water is lost during autoclaving.

The inset in Figure 2(b) displays the calibration curve that was used to correlate the spectrometer's light absorption measurements and PVB's water content. The latter, as we show later, is directly related to PVB's storage conditions in terms of water vapour chemical activity only. To create the chart, we measured the spectrum of several pre-presses including PVB sheets that were conditioned under different humidity levels, specifically at $a = 0.145, 0.25, 0.58$. The extremes were obtained by conditioning PVB within a dessicant box containing therein a saturated salt solution of either lithium chloride or calcium nitrate tetrahydrate respectively. The humidity of the enclosed air was ascertained by placing a hygrometer inside the box. Three samples per case were produced. For the middle activity level, i.e., $a = 0.25$, the humidity cabinet was employed and eleven samples were produced. In all cases, the PVB was conditioned for at least 72 hrs. Additionally, seven distinct measurements per sample were taken (midsection), with one reading every five millimeters, starting at 20 mm away from the edges.

Before the diffusion experiments, we took extra precautions to guarantee that the initial moisture profile in the samples was as homogeneous as possible. The pre-press samples were stored in the humidity cabinet and experimentation only took place once the coefficient of

variation ($CV = \sigma/\mu$) of the sample's moisture was less than 5%. This took approximately 25 days to achieve. From there, a moisture barrier (aluminum foil tape 425 by 3M) was placed on two edges of the glass.

To induce water diffusion in PVB, pre-press samples were placed inside a pre-heated convection oven. The oven's air supply was left open to avoid any pressure build-up, but most importantly, to maintain contact with the outside environment, thereby maintaining a constant vapor pressure. As we will discuss later, water may leave or enter the PVB foil as a function of the gradient of the surrounding atmosphere's chemical activity and PVB's conditioning regardless of temperature. By heating the pre-press samples in the oven, the chemical activity of the water vapor inside the oven decreased below the PVB's conditioning level since $P_{Sat}(T)$ is a monotonically increasing function of temperature. Consequently, we forced water to flow out from the PVB layer.

In terms of samples, four separate specimens were prepared. Two were probed at 100°C for 24hrs, while the remaining two were surveyed at 140°C for 16hrs. The samples were allowed to cool down to room conditions for 1-1.5hrs before taking any readings. The latter were taken from the edge in increments of 5 mm for a total of 10 points.

The diffusion cofficient was extracted from curves such as the one presented in Figure 2 (c). In similar fashion as Kapur et al.,[14] we employed Crank's[13] diffusion model for a semi-infinite plane:

$$C = C_1 + (C_o - C_1) \times erf\left(\frac{x}{2\sqrt{Dt}}\right) \tag{2}$$

where C is the concentration of water at a distance x, C_o is the initial concentration in the polymer, and C_1 is the concentration at the edge. When fitting the model, we assumed that C_1 was in equilibrium with the experimental room's vapor pressure. Moreover, we treated C_o and D as float variables. In this respect, the computed value for C_o differed at most by 2-5% compared to the experimental baseline taken before the experiments. This difference mirrors the moisture coefficient of variation within the samples, and therefore reflects experimental

uncertainty. Lastly, for the example in Figure 2 (c), $D = 1.5 \times 10^{-9}$ m^2s^{-1}.

Sorption & Solubility

The equilibrium mass from the DVS experiments was used to create sorption/desorption isotherms by plotting the ratio of the net mass—either gained or lost—by the polymer to the dry state. This is evidently equal to the amount of water sorbed/desorbed m_w divided by the dry mass m_{ref}. Figure 4 portrays sample sorption/desorption isotherms at 25°C. As seen in the image, the isotherms are non-linear and convex with the Henry limit at around $a \sim 0.5 - 0.6$ as previously reported in the literature.[6,9] We additionally show that hysteresis is negligible. Lastly, in the surveyed range $a = 0.1 - 0.9$, PVB can hold 0.1-3.1%wt.

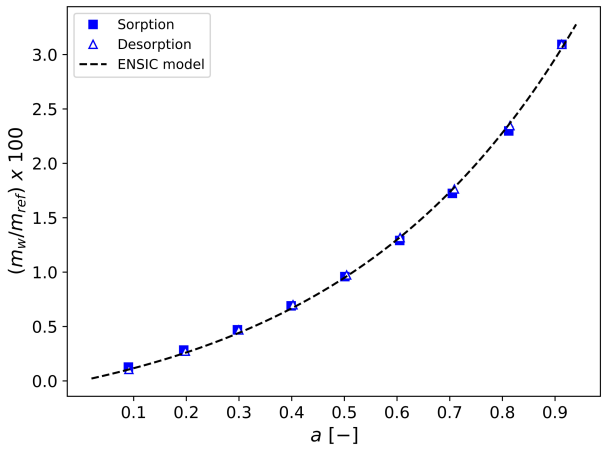

Figure 4: Sorption and desorption curve versus water chemical activity for RB41 at 25°C. The curves overlap indicating the absence of hysteresis in the sorption process. The dashed line is the ENSIC model as given in eq.5. The curve, being convex, mandates $k_s > k_p$, with the conclusion that water clusters in PVB at high chemical activities.

To overcome the temperature limitations of the DVS machine, we devised a static sorption technique to generate isotherms at higher temperatures. In our method, PVB samples of known moisture content were conditioned inside borosilicate glass flasks containing therein a sample holder, as well as ambient air and an aqueous solution of DI water with a chemically pure salt (table 1). The flasks were then heated inside a pre-heated convection oven while the salt solutions effectively set the humidity level of the enclosed air, and thus, the sorption of

water by the PVB sample. The flasks incorporated a special cap for pressure equalization that simultaneously prevented the exchange of moisture with the outside atmosphere. Finally, by comparing the change in mass of the PVB samples after heating, isotherms were created at 40, 60, 80°C.

The experimental protocol was as follows: PVB discs (diameter=40mm) were conditioned inside a humidity cabinet ($a = 0.25$ for at least 48hrs). The samples were then weighed (balance Kern ABJ, res. $\pm$0.1mg), and the dry mass approximated by subtracting the expected amount of water in the sample using Figure 4 (m_w/m_{ref} =0.41%wt for $a = 0.25$). We estimate an uncertainty equal to +0.1%wt, equivalent to $\Delta a = 0.05$, since the samples were briefly exposed to the atmosphere of the weighing room ($a = 0.43$). The uncertainty could have been reduced by assessing the sample's initial mass using a pre-weighed closed flask. Simultaneously, four flasks, each for housing a fresh PVB sample, were produced taking into account the variation of the salts' solubility with temperature (100-200ml). In this respect, the solubility varied 1.5-2 times in our temperature range.[15] We produced one flask per solution and let the latter rest for 48-72hrs. In the worst case, the measured activity at room conditions in the flasks did not differ by more than $\pm$0.04 compared to the figures from table 1, which was very well within the accuracy of the hygrometer used (TFA, res. $\pm$0.035). Thence, the flasks with the PVB discs were simultaneously heated to 40°C for a nominal period of 3 days, after which samples were expeditiously removed and promptly weighed. The process was repeated anew at 60°C, 80°C. When computing the isotherms, the equilibrium water activity was assumed to be in agreement with the literature at each temperature as per Ref.[15]

Table 1: Equilibrium water vapor activity for the different chemical salts used for static sorption[a]

Temperature [°C]	Lithium Chloride	Magnesium Chloride	Sodium Bromide	Sodium Chloride
25	0.1130	0.3278	0.5757	0.7529
40	0.1121	0.3160	0.5317	0.7468
60	0.1095	0.2926	0.4966	0.7450
80	0.1051	0.2605	0.5143	0.7558

[a] Equilibrium water vapor activity as found in Ref.[15]

Results & Discussion

Diffusion

Figure 5(a) summarizes the DVS results at 25°C and 40°C. In both cases, we observe that the diffusion coefficient decreases when increasing the water vapor chemical activity. Consequently, water molecules find it progressively difficult to diffuse through the polymer matrix when the water concentration is augmented. This decreasing relationship between D and a is typically a signature of attractive interaction between water molecules within the polymer, which often leads to cluster formation in the polymer matrix. [16,17]

We modeled this clustering effect using the empirical expression $D = D^* e^{\gamma \phi_s}$,[16] where D^* is presumably the diffusion coefficient at zero concentration, γ is thought of as a plasticization coefficient, and ϕ_s is the volume concentration of the gaseous species. Evidently, $\gamma < 0$ implies attractive interaction between water molecules via the polymer, which often results in clustering. From our data, we find $\gamma = -1.4$ at 25°C, where instead of ϕ_s we conveniently took the water vapor chemical activity a used to condition the PVB film. We observe no appreciable dependence of γ on temperature between 25°C and 40°C as shown by the similarity of the slopes of the fits of D with a for 25°C and 40°C (blue and red dashed lines in figure 5(a)). Consequently, as depicted in Figure 5(b), the activation energy of diffusion is constant regardless of chemical activity in this temperature range. From measurements taken at these two temperatures, we estimate $E_{d,avg} \approx 59$ kJ mol^{-1}, wherein we assumed an

Arrhenius behavior as is customary for most polymers.[18,19]

To put our value of the activation energy into perspective, we contrast our results to the literature concerning PVB. Kohl[7] gives the activation energy for diffusion as E_d=59 kJ mol^{-1} (25-35°C, gas permeation with mass spectrometry), Kim et al.[8] disclose 9 kJ mol^{-1} (20-50°C, Water Vapor Transmission Rate (WVTR) at $a = 0.6$, Illinois 7001), whereas Meitzner & Schulze[9] provide a rather low estimate of 19 J mol^{-1} (25-50°C, WVTR at $a = 1$, MOCON). Our own appraisal of their data, however, yielded 48.1 kJ mol^{-1}. While the specific PVB blend is rarely disclosed, all these authors worked with PVB for solar applications. The variability of the estimates should come as no surprise given the various commercial formulations and suppliers—all of which tend to be covered under the general umbrella of 'PVB'.

We propose to model the diffusion coefficient of water vapor D in PVB using a single expression combining the Arrhenius and plasticization effects:

$$ln(D/D_{ref}) = -\frac{E_d}{R_u}\left(\frac{1}{T} - \frac{1}{T_{ref}}\right) - \gamma(a - a_{ref}) \tag{3}$$

where the pre-exponential factor represents a reference state having a well-defined physical meaning. In this respect, $D_{ref} = 1 \times 10^{-11}$ m^2 s^{-1} is the diffusion coefficient at the reference temperature $T_{ref} = 25$°C and activity $a_{ref} = 0.0907$. The model performance has already been shown in dashed lines in Figure 5(a).

Continuing with the diffusion coefficients extracted via spectroscopy at 100°C and 140°C, Figure 6 depicts the results obtained thereof, plus the corresponding interpolated coefficients at 25°C and 40°C using eq. (3) ($a = 0.25$). The diffusion coefficients are plotted versus the reciprocal of temperature $1/T$. As seen in the image, the coefficients' trends exhibit different slopes depending on the temperature range, and hence, different activation energies. E_d varies from 59 kJ mol^{-1} (25-40°C) to roughly 29.2 kJ mol^{-1} (100-140°C). This variation of E_d with temperature induces a variation in D of two orders of magnitude over the temperature range tested: for $a = 0.25$ D= $7 \times 10^{-11} m^2/s$ at T=25°C whereas D= $1.6 \times 10^{-9} m^2/s$ at T=140°C.

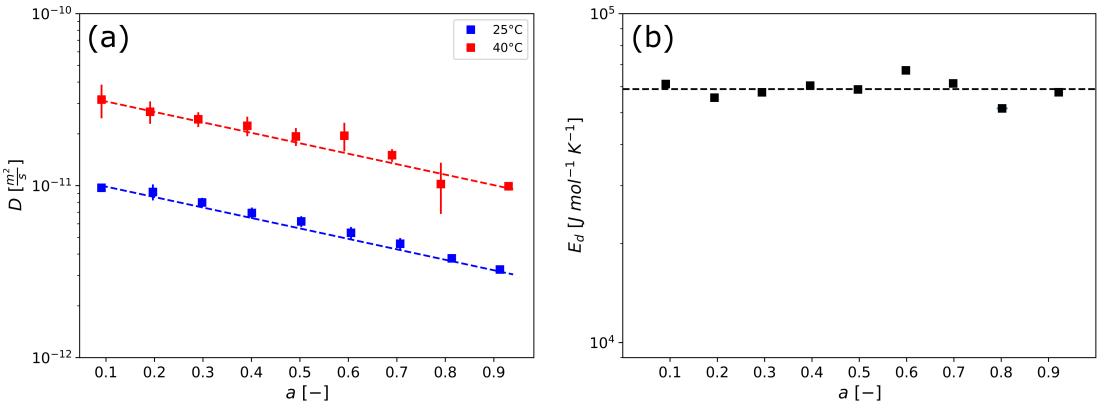

Figure 5: (a) Mean water diffusion coefficient in PVB at 25°C, 40°C against chemical activity. The vertical bars illustrate the negligible gap between the diffusion coefficients during sorption and desorption. (b) Activation energy as a function of chemical activity. The activation energy is computed using the data at 25°C and 40°C. Dashed line is the average energy $E_{d,avg} \approx 59$ kJ mol^{-1}.

By inspecting Figure 6, we visually estimate the inflection point of the activation energies to be around ∼72-75°C. This temperature range is much too low for any phase transition of water to take place under atmospheric conditions. Thus, we take that the variation in E_d reflects a change in the polymer itself. Indeed, DSC measurements by Elzière et al.[10] (20°C min^{-1}) support this notion. Said authors have found a wide exothermic signal around 50°C to 90°C with a marked peak at roughly 65-75°C that evidences a type of transition in PVB. As we discuss next, at elevated temperatures, the PVB polymer behaves akin to a viscous melt. Hence, a lower activation energy is expected since this state facilitates water diffusion in the polymer.

In a previous publication,[11] we have shown that it is possible to estimate the PVB state (glassy, rubbery, viscous melt) based on characteristic relaxation times provided that the temperature and time of solicitation are known. Of interest here is $t_d(T)$, the characteristic temperature-dependent time required for PVB to transition from the rubbery to the viscous state. We define the non-dimensional time $t_N = t_d(T)/t_{exp}$, (typically 10 days for DVS experiments, 16 hours for the spectrometry measurements at 140°C and 24 hours for those at 100°C). Whenever $t_N > 1$, PVB is assumed to be in the solid-like state. Conversely, for

$t_N < 1$ PVB is taken as being in the viscous, liquid-like state. For our DVS experiments, we find $t_N \approx 4.2$ (40°C), meanwhile, for the spectrometry measurements, we have $t_N \approx 4 \times 10^{-4}$ (100°C) and $t_N \approx 1.5 \times 10^{-5}$ (140°C). Thus, we may conclude that in the 40-100°C range, PVB exhibits transition states, which explains the variation in activation energy.

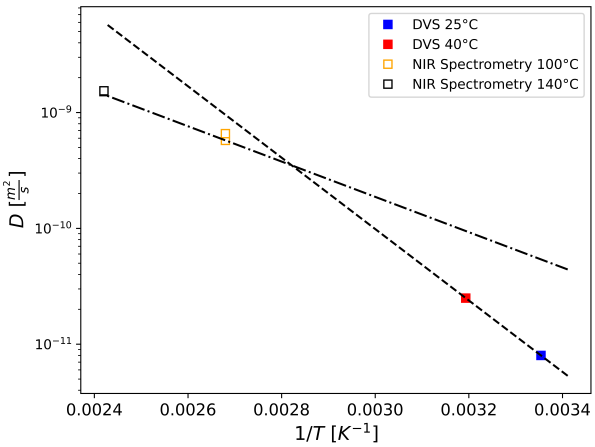

Figure 6: Water diffusion coefficient in PVB from DVS (25-40°C) and spectrometry (100-140°C) for $a = 0.25$

Sorption

Figure 7 depicts the sorption/desorption isotherms for water vapour in the PVB powder. The reference temperature was 25°C. As shown in Figure 7(a), in similar fashion to the PVB sheet, the isotherms are convex. Contrary to the latter case, however, hysteresis was significant for the powder. To put this into perspective, we cite the maximum difference between the isotherms was approximately equal to $\Delta m_w/m_{ref} = 0.304\%$ (8%wt -OH) and $\Delta m_w/m_{ref} = 0.692\%$ (18%wt -OH) coincidentally at the same activity level of $a = 0.6$. Most likely, the hysteresis reflects capillary bridges by water in the powder.

Continuing with the shape of the isotherms, Hauser & McLaren[6] together with Misra et al.[20] contend that the non-linear portion is the result of water clustering in PVB, a fact that coincides with our diffusion observations. For the sorption process, clustering means that as water molecules aggregate within the polymer, the clusters themselves attract increasing

quantities of water, thereby leading to a rapid increase in the sorption process.

Misra et al. also provided physical evidence of the clustering mechanism by showing one of its key features at high activity levels, i.e., increased polymer haziness due to the formation of two separate phases having unequal refractive indexes. To explain this behaviour, the authors logically proposed that hydroxyl groups (-OH) from the vinylalcohol monomer act as sorption sites. As the chemical activity increases, these sites become progressively filled. Water then forms clusters whenever all vacancies are exhausted. However, no direct experimental evidence linking hydroxyl group (-OH) concentration in PVB and water sorption was provided. To this end, Figure 7(b), where for clarity we have removed the desorption isotherms from Figure 7(a), provides the missing link. The figure clearly shows that the the higher the proportion of hydroxyl groups, the more water is sorbed.

The difference in sorption levels between the powder formulations appears to be a function of chemical activity. For illustrative purposes, at $a = 0.1$, the difference is relatively small, of about $\Delta m_w/m_{ref} = 0.11\%$. At $a = 0.9$, the gap widens explosively to $\Delta m_w/m_{ref} = 1.94\%$. Using the cluster perspective, we can image that the initial amount of water sorbed at low activity levels is linked to the amount of hydroxyl groups (-OH) in PVB. As the activity increases (e.g., $a > 0.5 - 0.6$), water clusters attract increasing amounts of water, thus widening the sorption gap between the powders.

We explain the relationship between water sorption and hydroxyl group (-OH) content qualitatively by considering that the interaction with water is by hydrogen bonding only since both molecules are highly polar. This means that we consider the interaction to be merely physical rather than chemical. Moreover, although we expect most hydroxyl groups to act as sorption sites, not every hydroxyl site would necessarily be involved in the sorption process because some hydroxyl groups (-OH) will invariably form hydrogen bonds between themselves. As the sorption sites are occupied, we assume that water, logically by hydrogen bonding, attracts increasing amounts of water when raising the chemical activity of the surrounding atmosphere.

Continuing with this idea of hydrogen bonding, the physical interaction would imply that sorption curves should scale with hydroxyl group concentration. Indeed, as shown in the inset of Figure 7(b), the sorption isotherms collapse onto a single curve when shifted vertically by a factor β_{OH}. For the inset, we arbitrarily selected the isotherm at 8%wt -OH as the reference. The proportionality between the sorption isotherms, as determined by the reciprocal of the shift factor ($1/\beta_{OH} = 1.79$) is smaller than the proportionality factor between the PVB blends in terms of hydroxyl group concentration (18/8=2.25). Therefore, consistent with our idea of hydrogen bonding, not every hydroxyl group appears directly involved in the sorption process.

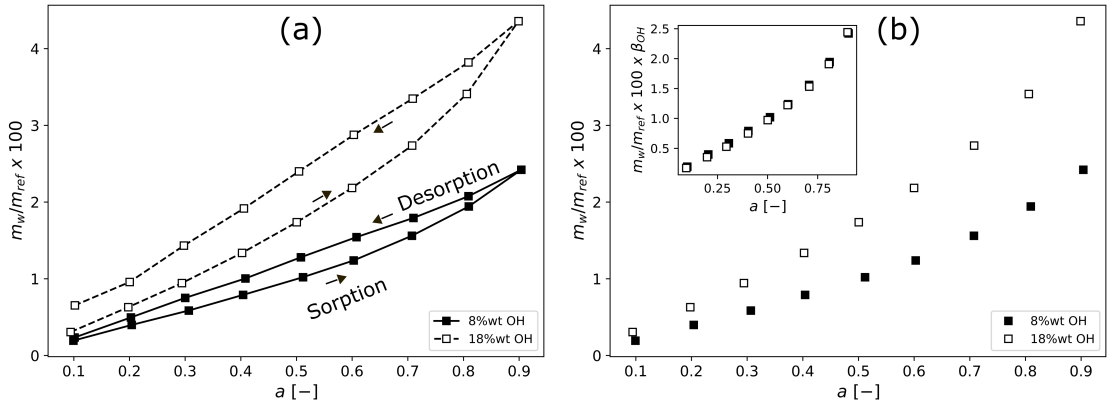

Figure 7: (a) Sorption and desorption isotherms for PVB in powder form at 25°C ; (b) Water uptake (sorption) as a function of chemical activity for different (-OH) group content in the PVB powders at 25°C. The inset shows that the curves can be shifted vertically to form a single curve using a factor β_{OH}.

To strengthen the case for hydrogen bonding, Figure 8 presents a comparison between our sorption isotherm for the PVB sheet and that of Hauser & McLaren[6] for unplasticized PVB (25°C, conditioning under acidic mixtures). Despite the differences in method and PVB composition, the isotherms elegantly overlap—a remarkable finding considering that unplasticized PVB is in the glassy sate ($T_g \approx 75$°C).[21] Hence, the polymer matrix, even in this highly constrained and complex state, appears to play a minimal role on water sorption. In this regard, the one similarity that stands out is the amount of hydroxyl groups, when accounting for the plasticizer in our case. In here, we have about 15%wt hydroxyl group

when including the extra plasticizer mass, compared to Hauser & McLaren's[6] 13%wt -OH. The sorption effect of the 2%wt -OH gap is probably simultaneously overshadowed by some hydrogen bonding with the plasticizer molecules, plus experimental error. Notwithstanding this minor issue, this result is further evidence that water molecules interact primarily with the polymer matrix through the OH groups and that the driving force for sorption is the -OH—H_2O, and H_2O—H_2O hydrogen bond interactions.

Description of Sorption Mechanism

Given the strong evidence for water clustering, both on the trends of D and the shape of the isotherms, we investigated several sorption models. As Meitzner & Schulze[9] did before us for an isotherm at 85°C, we found the *Engaged Species Induced Clustering* (ENSIC) approach to perfectly describe the isotherms for PVB.

The ENSIC sorption model is predicated on the assumption that sorption in a polymer matrix is Henry-like but nuanced by the inclusion of two proportionality constants k_p, k_s. The former describes the level of affinity of the sorbed molecules n_s towards polymer molecules n_p. The latter represents the gas affinity towards itself when dissolved within the polymer matrix.[22] In differential form:[22,23]

$$dn_s = (k_p n_p + k_s n_s)\ dP \tag{4}$$

where dn_s is the net amount of sorbed gas molecules by the polymer parting from a change in pressure dP. After integration, the model reads

$$\phi_s = \frac{e^{(k_s - k_p)a} - 1}{(k_s - k_p)/k_p}. \tag{5}$$

Where ϕ_s is the volume concentration of the sorbed gaseous species. The ENSIC model, via the relative values of k_s and k_p, can describe Flory-Huggins, Henry, or Langmuir type of isotherms. Most importantly for us, the model predicts clustering whenever $k_s > k_p$,

i.e., when the gaseous species display a stronger affinity towards themselves than towards polymer molecules.[22]

Figure 4 shows the numerical fit of the ENSIC model to the DVS data at 25°C for PVB in sheet form. For convenience, we present the model as fitted to the sorbed fraction of water $\phi_m = m_w/m_{ref}$ rather than the volume fraction ϕ_s as the former is the natural unit of our measurements. The error of this compromise is ultimately reflected on the magnitude of the individual constants, but the overall conclusion remained nonetheless the same. From a non-linear, least squares regression, we found $k_s^a = 3.25$ and $k_p^a = 1.04$, hence $k_s^a > k_p^a$. The same fit (not shown) using instead the volume fraction of dissolved water yielded $k_s = 2.21$ and $k_p = 0.01$, where we assumed that water dissolves in liquid form inside PVB. The values found therefore confirm the clustering of water and the strong affinity of water molecules amongst themselves in PVB at high activities.

More precisely, we apply the Zimm and Lundberg theory[24] to determine the likelyhood of clustering as well as the mean cluster size (MCS) of water molecules as a function of chemical activity in PVB from measured sorption isotherms.

The mean cluster size MSC, which is interpreted as the number of water molecules in the vicinity of another absorbed water molecule,[23,24] is defined as

$$MCS = (1 - \phi_s) \left[\frac{\partial \ln \phi_s}{\partial \ln a} \right]_{P,T} - 1 \tag{6}$$

Under the ENSIC framework, it writes as:[23]

$$MCS = \frac{(1 - \phi_s)(k_2\phi_s + 1)\ln(k_2\phi_s + 1)}{k_2\phi_s} \tag{7}$$

where $k_2 = (k_s - k_p)/k_p$ is determined from the ENSIC model parameters when fitted to the volume fraction ϕ_s. $MCS > 1$ signals clustering of water in the polymer.[25]

For PVB, the MCS trend is quasi-linear with respect to the chemical activity (not shown), starting at 1.1 at low activity values ($a \sim 0.1$) and increasing to 2.2 at high activities

($a \sim 0.9$). Thus, MCS computation reveals that clusters of water start to form in PVB even at small chemical activity.

Role of Temperature

Figure 8 depicts the sorption isotherms for PVB in sheet form from 25°C to 60°C, plus two isotherms from the literature, to wit, the already discussed isotherm from Hauser & McLaren[6] at 25°C, plus a curve from Meitzner & Schulze[9] for solar grade PVB (Trosifol R40, conditioning with humidity cabinet, water measurements via chemical titration). From the information we gathered, the main chemical make-up of this solar PVB blend comprises 2% vinylacetate groups, 22% vinylalcohol groups, and 76% vinylbutyral. A plasticizer molecule, in an apparent proportion of 20-30% is used.[26] Thus, the solar grade is similar enough to the one used here.

Before proceeding, we duly remark that measurements at 80°C (static sorption) yielded negative sorption values at low levels of chemical activity. We performed additional experiments at this temperature with fresh samples and observed a correlation between the residence time in the oven and the vertical downwards shift of the isotherms towards negative sorption. Consequently, we concluded that at this temperature PVB either degrades or loses rapidly other compounds besides water if exposed to oxygen from the atmosphere and therefore did not present any results at this temperature.

Returning to the isotherms, all the curves overlap in spite of experimental method, PVB state (rubbery or glassy), grade (classical PVB for glass or solar blend), or temperature. To the best of our knowledge, this remarkable result has not been discussed anywhere else. Moreover, in a further nod to the role of hydrogen bonding in the sorption process, the solar grade PVB does not exhibit any particular divergence from the other isotherms, despite including additives for solar performance.

The collapse of the curves hides an important fact: the solubility of water in PVB is a *decreasing* function of temperature. When raising the temperature arbitrarily from T_1 to T_2,

the partial vapor pressure of water must likewise increase to maintain the chemical activity level since

$$a(T_1) = \frac{p_w^{T_1}}{P_{Sat}(T_1)} = \frac{p_w^{T_2}}{P_{Sat}(T_2)} = a(T_2) \rightarrow p_w^{T_2} = p_w^{T_1} \frac{P_{Sat}(T_2)}{P_{Sat}(T_1)}$$

and P_{sat} is a monotonically increasing function of temperature. In other words, the collapse of the isotherms in Figure 8 implies that to solubilize equal amounts of water in PVB when raising the temperature, it is equally necessary to increase the vapor pressure, hence, the solubility must decrease. To better show this fact, the inset in the figure portrays the water sorbed by PVB against vapor pressure, whence the reduction in solubility is clearly visible. To ease the comparison, the inset further depicts the Henry solubility slopes ($a \leq 0.55$, dashed lines) for each temperature (for clarity, we only show the DVS curves). As seen in the inset, the slope at 40°C is evidently smaller than the corresponding one at 25°C.

The behavior of water in PVB is quite interesting since the loss in solubility with temperature appears to be perfectly balanced by the respective increase in the vapor pressure of water regardless of the polymer structure. Thus, the interaction between water in the surrounding atmosphere and dissolved water in PVB is akin to that between ordinary water in the gaseous and liquids states. Surely, this is a reflection that water in PVB interacts mostly by hydrogen bonding, not by chemical means.

Figure 8 (b) presents the solubility of water versus $1/T$ in the Henry limit ($a \leq 0.55$). To construct the figure, we complemented our solubility measurements from 25°C to 60°C with estimates from the literature previously referenced when discussing Figure 8. In all cases, we employed a linear regression and took the slope of the curves as the solubility. Overall, the data shows an Arrhenius behavior. From the DVS results, the slope of the curve, which represents the heat of solution is roughly $\Delta H_s \approx -42$ kJ mol^{-1}. By including the remaining solubility estimates, we find approximately $\Delta H_s \approx -44.4$ kJ mol^{-1}. The reference solubility at 25°C is 5.96×10^{-3} kg m^3 Pa^{-1}.

The computed heat of solution is contrary to the one appraised by us from Kohl et al.[7]

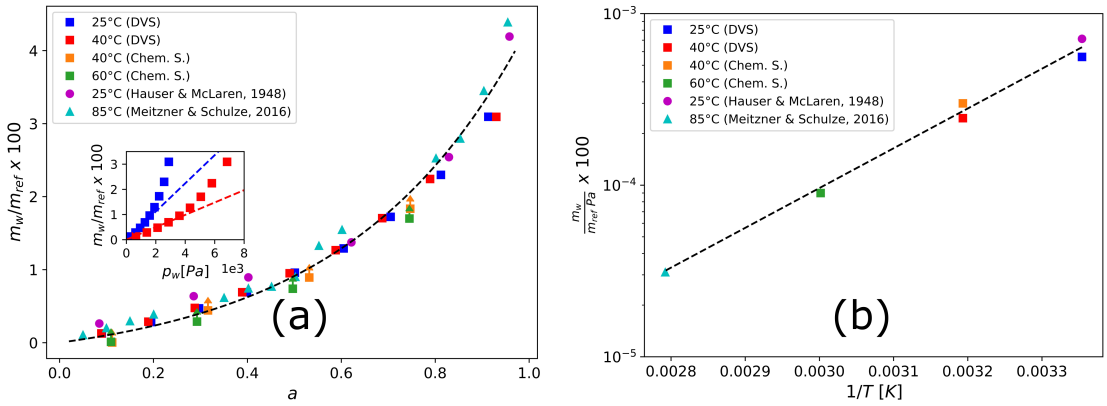

Figure 8: (a) Sorption isotherms for PVB including data from the DVS and static sorption methods between 25°C to 60°C, plus two additional isotherms from the literature. Regardless of temperature, formulation, or PVB state, the isotherms form a single curve when plotted against water vapor chemical activity. For the static sorption data, the caret symbol illustrates the direction and magnitude of the uncertainty inherent in the method. In the spirit of completeness, the dashed line is the ENSIC fit across all isotherms ($k_s = 3.53$, $k_p = 0.87$). The inset depicts the sorption of water as a function of vapor pressure for 25°C (blue symbols) and 40°C (red symbols), wherein the loss of solubility with temperature is observed. The slopes of two dashed lines (that represent the linear interpolation of the data for $a \leq 0.55$) give the Henry solubility. (b) Arrhenius law for water vapour solubility in PVB.

(mass spectrometry, unknown PVB, $\Delta H_s = 7.80$ kJ mol^{-1}), but in agreement, in terms of sign, with Kim et al.[8](WVTR, unknown PVB, $\Delta H_s = -8.74$ kJ mol^{-1}). In this respect, the closest estimate to our results is given by Hauser & McLaren[6] (unplasticized PVB, $\Delta H_s = -54.4$ kJ mol^{-1}).

It should be noted that the heat of solution computed in the present work is remarkably close to the heat of vaporization of pure water which is, in this temperature range, between 43.99 kJ mol^{-1} and 41.58 kJ mol^{-1}. This is further confirmation of the vision proposed in the present work: the sorption of water by PVB is mainly promoted via H-bonding interaction. Even though two types of H-bonds have been discussed—between the OH groups of the polymer and the water molecules at low chemical activity and between water molecules via the growth of water clusters at high chemical activity—at first order, it is always a matter of either forming or breaking H-bonds, hence the similarity between the heat of solution and vaporization values.

To close this section, we discuss some important implications of our work. First of all, the effect of temperature is subtle. What matters most when conditioning PVB is not the conditioning temperature, but the gradient between the chemical activity of water in the surrounding atmosphere and the amount of water dissolved in the PVB polymer. If the gradient is positive (e.g., the chemical potential of water is higher in the atmosphere than in PVB), water will diffuse inwards through the polymer irrespective of temperature. This is what occurs in the typical aging tests of solar panels. The opposite is evidently true as we have shown via our spectrometry measurements, and would correspond to the bake testing of glass (100°C, 16hrs). Thus, an increase in conditioning temperature accelerates the water diffusion process, but does not directly control the direction of water flow. Furthermore, to limit PVB degradation, temperatures above 60°C should be avoided.

Second, our findings reveal that issues of bubbles or blisters may be richer than anticipated in the literature. In this respect, a brilliant mechanism for blister growth has been numerically shown in the literature for EVA.[2] As water enters the polymer, it degrades the

adhesion level between the polymer and the glass, thus leading to blister growth by delamination. Evidently, the same mechanism would apply to PVB as adhesion is also moisture dependent.[3] In light of our results, bubbles/blister formation is suppressed whenever there is zero flux at the polymer's edge. However, bake test studies in our laboratory reveal that bubbles/blisters do form even in the absence of water ingress. In this case, water actually escapes from the PVB layer since the chemical activity of the surrounding atmosphere falls below the concentration of water in PVB upon heating and eventually fills small gas inclusions present at the interface between the glass and the polymer. Therefore, a plurality of mechanisms may be simultaneously at play: the transfer of water can increase the pressure in small gas inclusions while reducing polymer glass adhesion. These two combined effects can lead to the appearance of centimetric blisters, clearly visible on solar panels or laminated glass. Third, our results can be used to devise solutions to issues faced in the manufacturing of glass assemblies with PVB. For example, if PVB is mistakenly conditioned at a higher humidity than intended, one could employ moderate temperatures and a dry atmosphere to force the excess water out. Evidently, the feasibility of such an strategy must be weighed against costs and time constraints.

Conclusion

The diffusion and sorption experiments presented in this work were carried out using different experimental techniques and varying the various parameters of interest (chemical activity of the surrounding vapor, temperature and characteristic measurement time) over the widest possible measurement range. This has enabled us to produce a substantial dataset for sorption and diffusion coefficient, and to produce robust fits of these quantities with these parameters, which is likely to be useful for future work. In addition to this practical aspect, the quality of the data obtained enabled us to compare the results obtained with theoretical models in the literature. The following lessons can be drawn from this comparison of ex-

perience and theory. Firstly, diffusion is an energetically activated process. The activation energy measured depends on the state of the polymer (rubber, viscous). For these complex systems, the state of the polymer obviously depends on temperature, but also to a lesser extent on the characteristic duration of solicitation. This suggests that non-trivial effects may be observed, which could explain the variability of results in the literature. Secondly, water solubility in PVB depends not only on the chemical activity of the surrounding vapour, but also on the abundance of hydroxyl groups in the polymer. The data obtained are very well described by the ENSIC (Engaged Species Induced Clustering) model, and the extracted constant values suggest clustering with a MCS (Mean Cluster Size) larger than one over the entire chemical activity range. In addition, the temperature dependence enables us to extract the heat of solution, which is found to be extremely close to that of simple liquid water, thus corroborating the image of clustered water organization within the polymer.

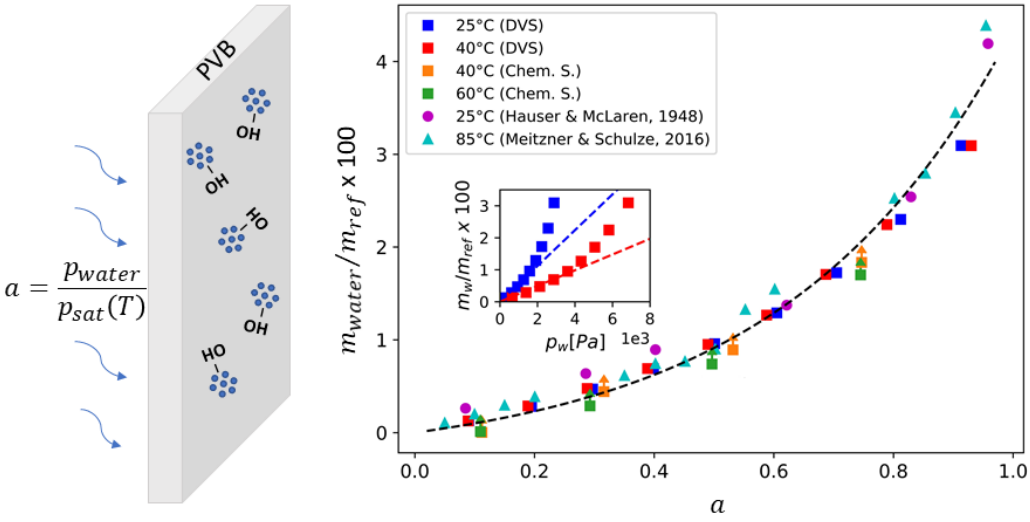

Figure 9: TOC Graphic

Acknowledgement

The authors thank Lionel Bureau, Jérôme Giraud, Diamante Macé and Guillaume Dupeux for their valuable help as well as an anonymous referee for his/her interesting suggestions. This study was funded by Saint-Gobain Research Paris.

References

(1) Allan, S. M. *Energy Saving Glass Lamination via Selective Radio Frequency Heating*; 2012.

(2) Gagliardi, M.; Paggi, M. Multiphysics analysis of backsheet blistering in photovoltaic modules. *Solar Energy* **2019**, *183*, 512–520.

(3) Keller, U.; Mortelmans, H. Adhesion in laminated safety glass–what makes it work. Glass processing days. 1999; pp 353–356.

(4) Desloir, M.; Benoit, C.; Bendaoud, A.; Alcouffe, P.; Carrot, C. Plasticization of poly (vinyl butyral) by water: Glass transition temperature and mechanical properties. *Journal of Applied Polymer Science* **2019**, *136*, 47230.

(5) Botz, M.; Wilhelm, K.; Siebert, G. Experimental investigations on the creep behaviour of PVB under different temperatures and humidity conditions. *Glass Structures & Engineering* **2019**, *4*, 389–402.

(6) Hauser, P. M.; McLaren, A. D. Permeation through and sorption of water vapor by high polymers. *Industrial & Engineering Chemistry* **1948**, *40*, 112–117.

(7) Köhl, M.; Angeles-Palacios, O.; Philipp, D.; Weiβ, K.-A. *Service Life Prediction of Polymeric Materials*; Springer, 2009; pp 361–371.

(8) Kim, N.; Han, C. Experimental characterization and simulation of water vapor diffusion through various encapsulants used in PV modules. *Solar energy materials and solar cells* **2013**, *116*, 68–75.

(9) Meitzner, R.; Schulze, S.-H. Method for determination of parameters for moisture simulations in photovoltaic modules and laminated glass. *Solar Energy Materials and Solar Cells* **2016**, *144*, 23–28.

(10) Elzière, P.; Fourton, P.; Demassieux, Q.; Chennevière, A.; Dalle-Ferrier, C.; Creton, C.; Ciccotti, M.; Barthel, E. Supramolecular structure for large strain dissipation and outstanding impact resistance in polyvinylbutyral. *Macromolecules* **2019**, *52*, 7821–7830.

(11) Arauz Moreno, C.; Piroird, K.; Lorenceau, E. Extended time–temperature rheology of polyvinyl butyral (PVB). *Rheologica Acta* **2022**, *61*, 539–547.

(12) Corroyer, E.; Brochier-Salon, M.-C.; Chaussy, D.; Wery, S.; Belgacem, M. N. Characterization of commercial polyvinylbutyrals. *International Journal of Polymer Analysis and Characterization* **2013**, *18*, 346–357.

(13) Crank, J. *The mathematics of diffusion*; Oxford university press, 1979.

(14) Kapur, J.; Proost, K.; Smith, C. A. Determination of moisture ingress through various encapsulants in glass/glass laminates. 2009 34th IEEE Photovoltaic Specialists Conference (PVSC). 2009; pp 001210–001214.

(15) Greenspan, L. Humidity fixed points of binary saturated aqueous solutions. *Journal of research of the national bureau of standards* **1977**, *81*, 89–96.

(16) Favre, E.; Schaetzel, P.; Nguygen, Q.; Clement, R.; Neel, J. Sorption, diffusion and vapor permeation of various penetrants through dense poly (dimethylsiloxane) membranes: a transport analysis. *Journal of Membrane Science* **1994**, *92*, 169–184.

(17) Barrie, J. A.; Platt, B. The diffusion and clustering of water vapour in polymers. *Polymer* **1963**, *4*, 303–313.

(18) Barrer, R.; Rideal, E. K. Permeation, diffusion and solution of gases in organic polymers. *Transactions of the Faraday Society* **1939**, *35*, 628–643.

(19) Van Amerongen, G. J. The permeability of different rubbers to gases and its relation to diffusivity and solubility. *Journal of Applied Physics* **1946**, *17*, 972–985.

(20) Misra, A.; David, D.; Snelgrove, J.; Matis, G. Clustering of absorbed water in amorphous polymer systems. *Journal of applied polymer science* **1986**, *31*, 2387–2398.

(21) Cascone, E.; David, D.; Di Lorenzo, M.; Karasz, F.; Macknight, W.; Martuscelli, E.; Raimo, M. Blends of polypropylene with poly (vinyl butyral). *Journal of applied polymer science* **2001**, *82*, 2934–2946.

(22) Favre, E.; Nguyen, Q.; Clément, R.; Néel, J. The engaged species induced clustering (ENSIC) model: a unified mechanistic approach of sorption phenomena in polymers. *Journal of membrane science* **1996**, *117*, 227–236.

(23) Favre, E.; Clément, R.; Nguyen, Q. T.; Schaetzel, P.; Néel, J. Sorption of organic solvents into dense silicone membranes. Part 2.—Development of a new approach based on a clustering hypothesis for associated solvents. *Journal of the Chemical Society, Faraday Transactions* **1993**, *89*, 4347–4353.

(24) Zimm, B. H.; Lundberg, J. L. Sorption of vapors by high polymers. *The Journal of Physical Chemistry* **1956**, *60*, 425–428.

(25) Modesti, M.; Dall'Acqua, C.; Lorenzetti, A.; Florian, E. Mathematical model and experimental validation of water cluster influence upon vapour permeation through hydrophilic dense membrane. *Journal of membrane science* **2004**, *229*, 211–223.

(26) Schulze, S. Charakterisierung polymerer Zwischenschichten in Verbundglas-Solarmodulen. Ph.D. thesis, Martin–Luther–Universitität Halle–Wittenberg, Germany, 2011.